Supporting Information for

Chiral Hydrogen Bond Enviroment Providing Unidirectional Rotation in Photoactive Molecular Motors

Cristina García-Iriepa,[1] Marco Marazzi,[1] Felipe Zapata,[1] Alessio Valentini[1], Diego Sampedro[2,] and Luis Manuel Frutos[1,*]*

[1] Departamento de Química Física, Universidad de Alcalá, E-28871 Alcalá de Henares, Madrid, Spain.

[2] Departamento de Química, Centro de Investigación en Síntesis Química (CISQ), Madre de Dios, 51, E-26006, Logroño, Spain.

Contents:

1. Computational Details.

The ground state minima were found at the Møller-Plesset to second order (MP2) level of theory. Frequency calculations of these stationary points were performed in order to confirm its nature. The most stable ground state conformation was selected as the starting structure for the complete photochemical study, performed at Multi-State Complete Active Space Perturbation to Second Order with a Complete active Space Self Consistent Field reference wavefunction (i.e. MS-CASPT2//SA-CASSCF methodology)[1,2]. This methodology was already shown to successfully describe the photochemistry of several molecular systems[3]. For this study, the *State Averaged-Complete Active Space Self Consistent Field* (SA-CASSCF) method[1] was employed for the calculation of the electronic transitions and the computed minimum energy paths, suing in all the cases four states (S_0, S_1, S_2 and S_3) with same weight in the averaged wavefunction. The active space chosen comprises all the π and π* orbitals (8 electrons in 8 orbitals).

The minimum energy paths were calculated from the Franck–Condon structure at the excited electronic state with the higher oscillator strenght (i.e. S_3), by using the steepest descent algorithm (step-size between 0.02 and 0.05 Bohr). The characterization of the electronic state crossings found along the minimum energy paths was performed at the CASSCF level, determining for each case the two non-adiabatic coupling vectors defining the branching plane (Gradient Difference (GD) and Derivative Coupling (DC) vectors). In order to characterize the topology of the crossing (sloped, peaked, etc.)[4] a scan of 20 geometries around the conical intersection was generated by linear combination of

the GD and DC vectors, determining for each point of the scan the energies of the involved electronic states at the SA-CASSCF level.

Lastly, energy correction including dynamic correlation for the most relevant structures along the reaction paths was performed at the MS-CASPT2 level of theory.

The MP2 conformational study and the calculation of GD and DC vectors were performed with the Gaussian 09 software.[5] Whereas, MOLCAS 7 (version 7.6) package was used for the calculation of the minimum energy paths and CASPT2 single point energy corrections.[6]

2. S_3 State Unidirectional Rotation: Torsional Profiles.

Molecular motors are characterized by a controlled unidirectional rotation whereas molecular switches perform a non controlled rotation.

The unidirectionality of the rotation after excitation of the proposed molecular motor has been proven (see main text) by means of dynamics calculations. This property was also analyzed by determining the energy barrier for the opposite rotation in S_3.

A relaxed scan along the torsion coordinate (fixing the dihedral representative of the torsion, φ) at SA-CASSCF level was performed in S_3. The results show an energy barrier of ca. 3 kcal/mol in this state, being necessary a rotation from -7.3 degrees (Franck–Condon structure) to 13.7 degrees to reach this structure. Therefore, the molecule has to rotate at least ca. 21 degrees in order to abort the unidirectional rotation. On the other hand, for the molecular switch model, it is found that reversion of the rotation can be achieved with only 15 degrees of rotation, at almost the same cost of energy (ca. 3 kcal/mol), therefore decreasing the unidirectionality character (Figure 1S).

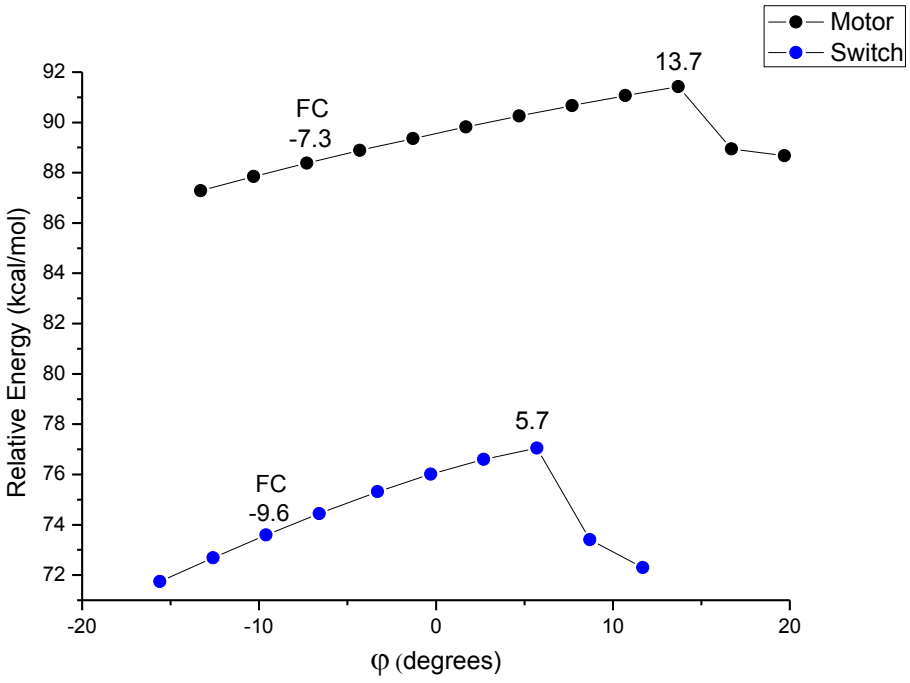

Figure 1S. Relaxed scan along the torsion coordinate with the energy barrier in S_3 needed to abort the unidirectional rotation. (FC corresponds to the Franck–Condon geometry).

In order to further analyze the initial direction of rotation after optical excitation, and therefore the preference of the system for the unidirectional rotation, we have studied the dynamics after excitation to S_3 state for a short simulation time (*i.e.* 20 fs). Sampling ground state initial conditions following a Maxwell–Boltzmann distribution at 300 K, a total of 300 trajectories were computed following a local expansion of the potential energy surfaces in both ground and excited states (Section 7 for methodological details). The average carbon-carbon central bond torsion (φ), tends to reduce its angle in the clockwise direction, and no branching or significant population is shifted to increasing angles (see Figure 2S).

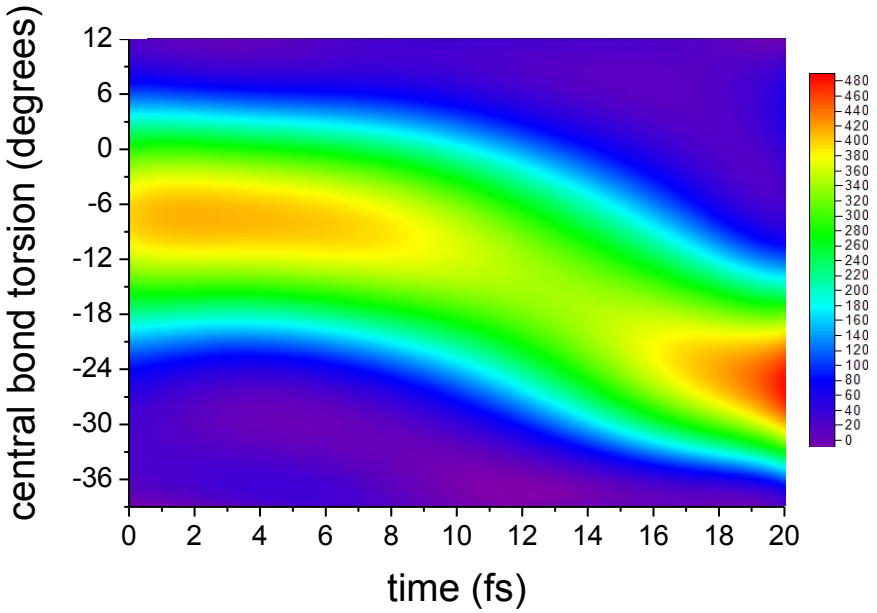

Figure 2S. Density population for an ensemble of 300 trajectories on S_3 after vertical excitation as a function of time and central bond torsion (φ). The density population is indicated by colors, where the color scale provides the number of points per degree and fs obtained from the 300 trajectories. The evolution of the trajectories shows the unidirectional rotation after excitation to S_3.

3. Molecular Motor Absorption Spectrum.

The absorption spectrum was computed at the MS-CASPT2//SA-CASSCF level of theory for the most stable ground state conformer (see section 3).

The UV-Visible absorption spectrum shows a $S_0 \rightarrow S_1$ transition at 61.7 kcal/mol (48.6 kcal/mol at CASPT2 level), a $S_0 \rightarrow S_2$ transition at 115.5 kcal/mol (102.2 kcal/mol at CASPT2 level) and a $S_0 \rightarrow S_3$ transition at 121.8 kcal/mol (98.4 kcal/mol at CASPT2 level). All these excited states exhibit a dominant $^1(\pi,\pi^*)$ electronic configuration but, only for S_2 and S_3 the orbitals (occupied and virtual) involved in the excitation are centered on the central carbon atoms, being S_3 the state that exhibit a larger participation of this transition. The shape of the orbitals involve in the excitation to S_3 indicates the rupture of the central double bond after excitation (Figure 3S).

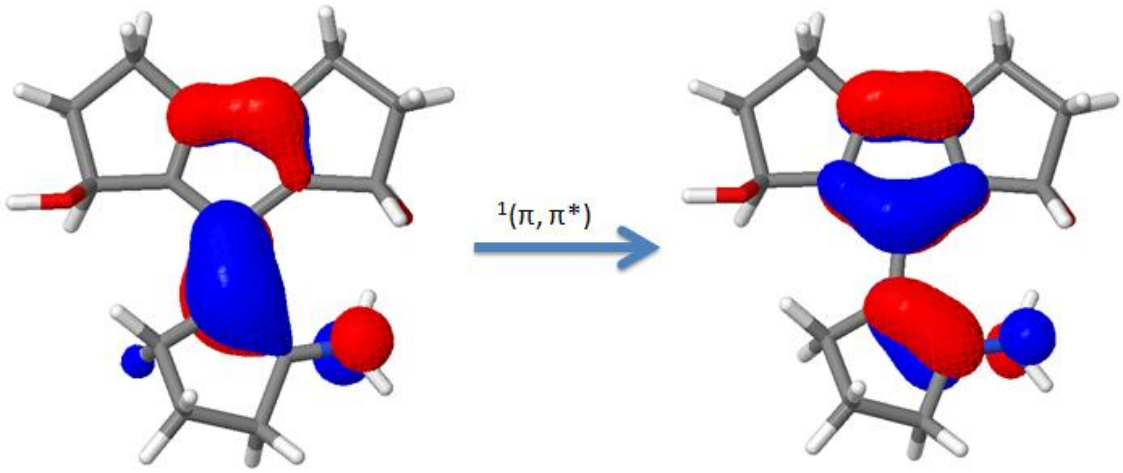

Figure 3S. CASSCF molecular orbitals describing the highest weight configuration ($^1(\pi,\pi^*)$ central double bond exitation) for the two lowest-lying optically bright states of the system (S_2 and S_3).

In addition, oscillator strength values for the electronic transitions aforementioned were calculated in order to identify the bright state/s. It was found that the $S_0 \rightarrow S_2$ and $S_0 \rightarrow S_3$ transitions exhibit higher oscillator strength (0.32 and 0.35 respectively).

4. Branching Space Characterization of Conical Intersections.

Along the reaction path (S_3 to S_0), three main conical intersections (S_3/S_2 CI, S_2/S_1 CI and S_1/S_0 CI) were found. All these crossings were characterized at CASSCF level. In the main text the topology of each crossing is shown, while here both, Gradient Difference (GD) and Derivative Coupling (DC) vectors calculated for each crossing, are displayed (Figure 4S).

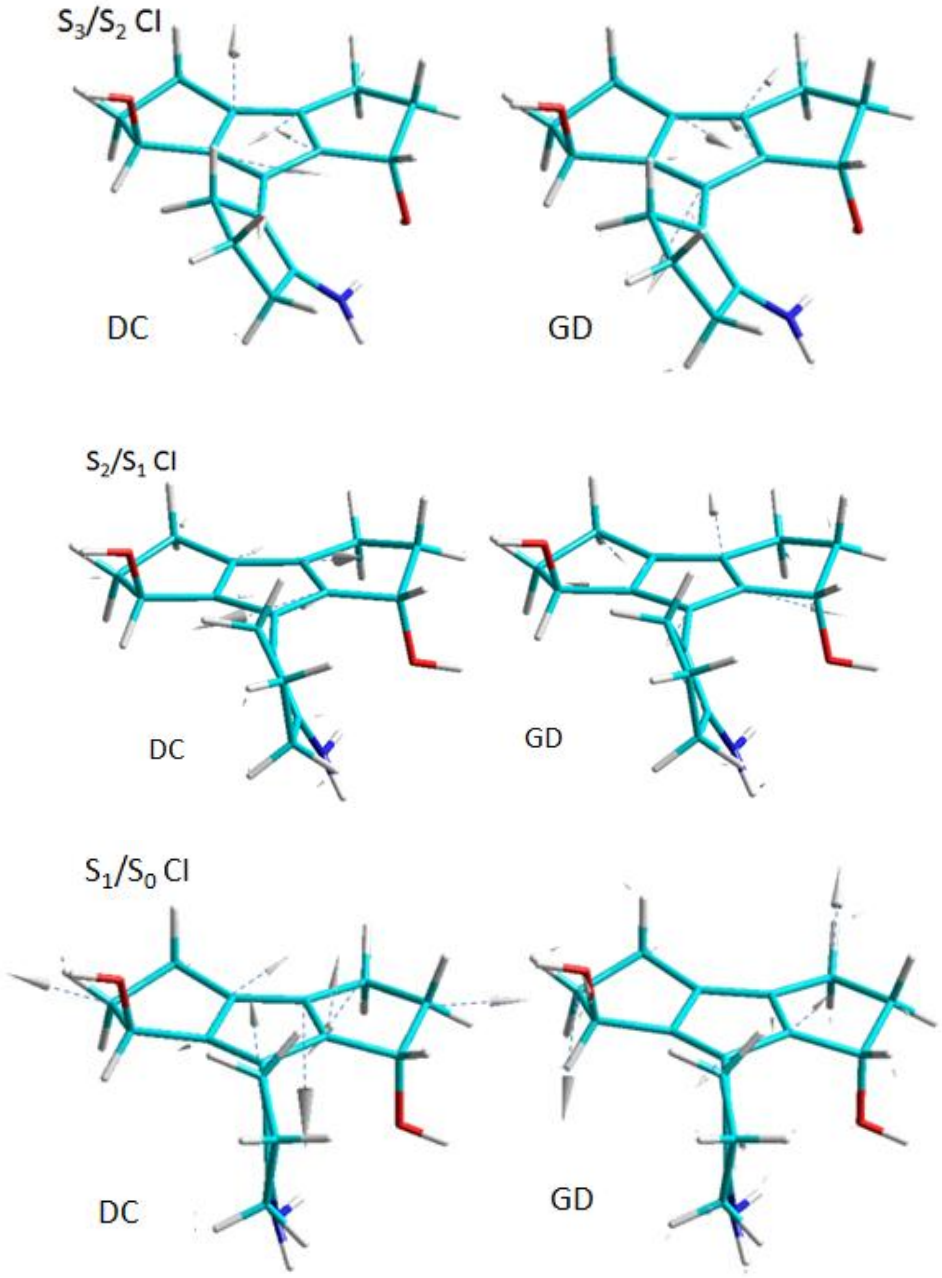

Figure 4S. Conical intersection characterization: non-adiabatic coupling vectors, DC and GD vectors, for the CIs described in the main text (Figure 3 and 4).

5. Minimum Energy Path From S_1/S_0 Conical Intersection.

From the S_1/S_0 conical intersection, the system can decay to the ground state by two different paths: one completion the 180 degrees cycle and the other one aborting the torsion. In both cases, the same initial structure is recovered.

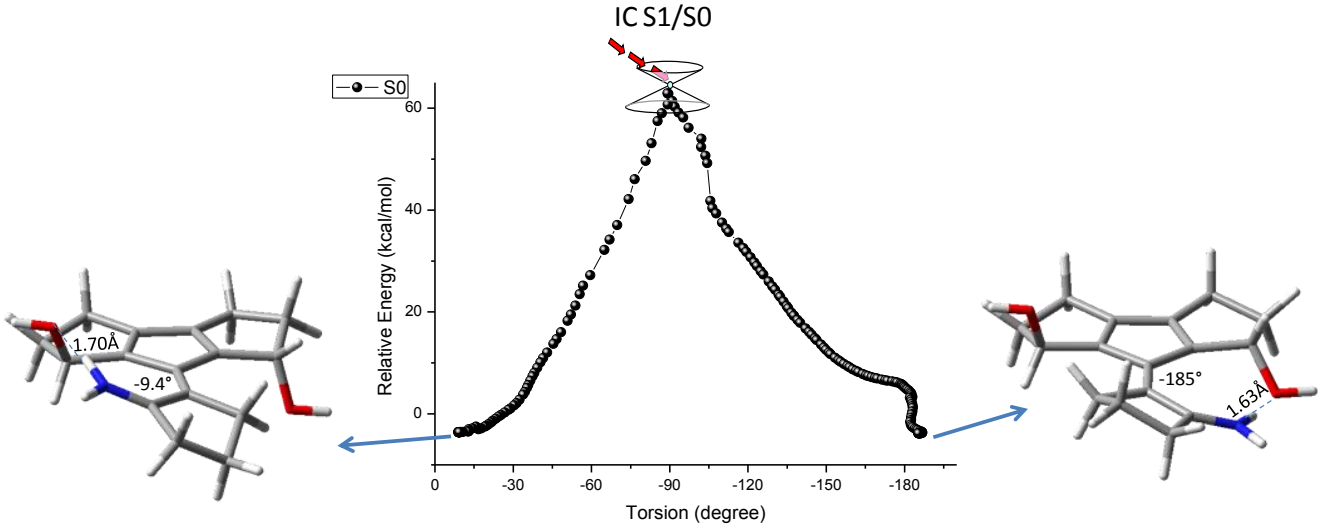

Figure 5S. Ground state minimum energy paths from S1/S0 CI in the direction defined by the two steepest valleys emerging from the tip of the CI. Complete rotation is fulfilled following the favored path, while inversion of the rotation is also possible but unfavorable, recovering the system its initial structure.

6. CASPT2//CASSCF Energy Profile.

CASPT2 single point energy corrections were calculated for the most representative structures found along the minimum energy paths. As shown in Figure 6S, a good agreement between CASSCF and CASPT2 relative energies (with respect to the Franck–Condon ground state structure) is found.

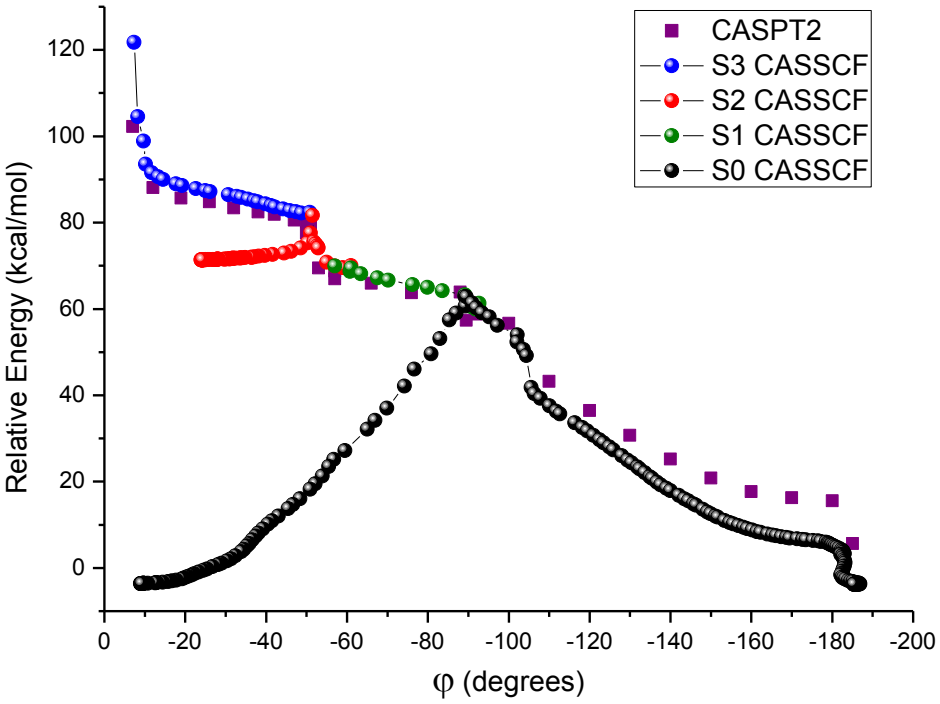

Figure 6S. CASPT2 single point energy corrections along the CASSCF MEP.

7. Methodology for Ground State Sampling and Franck-Condon Initial Rotation Dynamics with Analytical Potential Energy Surfaces.

The molecular dynamics simulations at constant temperature were carried out using a Nose−Hoover chain of thermostats, applying a time reversible integrator, as has been discussed elsewhere. [7-9] To describe the forces in the surroundings of the Franck−Condon point, the S_0 potential energy surface (PES) was built by second-order expansion of the energy E as a function of internal coordinates:

$$E(\boldsymbol{q}-\boldsymbol{q}_0) \approx E(\boldsymbol{q}_0) + \boldsymbol{g}\,(\boldsymbol{q}-\boldsymbol{q}_0) + \frac{1}{2}\,(\boldsymbol{q}-\boldsymbol{q}_0)^T\,\boldsymbol{H}\,(\boldsymbol{q}-\boldsymbol{q}_0) \qquad \text{Eq. 1}$$

where $\boldsymbol{q}_0$ is the vector represents the ground state equilibrium structure, $\boldsymbol{q}$ is the position vector in internal coordinates at any time, $\boldsymbol{g}$ is the energy gradient (*i.e.* the first derivative of the energy with respect to the position vector) and $\boldsymbol{H}$ is the Hessian matrix (*i.e.* the second derivative of the

energy with respect to the position vector), being both $\boldsymbol{g}$ and $\boldsymbol{H}$ calculated in the expansion point. Therefore, an analytical energy gradient expression is obtained by deriving eq.1:

$$\nabla E(\boldsymbol{q}) \approx \boldsymbol{g_q} = \boldsymbol{g}\,(\boldsymbol{q}_0) + \ \boldsymbol{H}\,(\boldsymbol{q} - \boldsymbol{q}_0) \qquad \text{Eq. 2}$$

Using the previous expansion and the Wilson $\boldsymbol{B}$ matrix,[10] which contains the derivatives of the internal coordinates with respect to the Cartesian coordinates with elements of the form $B_{ij} = \frac{\partial q_i}{\partial x_j}$, an analytical expression for the energy gradient in Cartesian coordinates is obtained:

$$\boldsymbol{g_x} = \boldsymbol{B^T}\,\boldsymbol{g_q} \qquad \text{Eq. 3}$$

For initializing the simulation at the desired temperature, it was implemented a pseudo-random number generator for supplying initial random velocities belonging to a Maxwell−Boltzmann distribution for the given temperature.[11] An integration step of 0.1 fs was applied.

For sampling the phase space at the S_0 minimum (Franck−Condon geometry), the forces were obtained using the Hessian matrix calculated at the minimum, where the energy gradient is just a null vector. Using the methodology described above, a trajectory of 1 ns in the surroundings of the Franck−Condon point was simulated on the S_0 PES, recording all positions and momenta at each step of integration. From these data, 300 random geometries (with their respective momenta) were selected and vertically excited to the S_3 electronic state. The simulation was then continued on the S_3 PES, in order to describe the dynamical behavior after $S_0 \rightarrow S_3$ vertical excitation. The S_3 PES was also built by second-order expansion (Eqs. 1, 2, 3), calculating the Hessian matrix for the Franck−Condon geometry. All 300 S_3 trajectories were performed for 20 fs (initial relaxation trajectories) with integration step of 0.1 fs, recording the variations of φ angle (Figure 3 in main text).

8. CASSCF(8,8)/6-31G* vs CASSCF(8,8)/3-21G*Energy Profiles Along the CASSCF(8,8)/6-31G* Minimum Energy Path.

In order to study the molecular dynamics of the photoactive molecular motor, a preliminary study with a smaller basis set (3-21G) has been proposed due to the large computational cost of the on-the-fly dynamics. Nevertheless, the validity of the CASSCF(8,8)/3-21G results is conditioned by the accuracy of these calculations in describing the 6-31G* potential energy surfaces.

Therefore, it becomes mandatory to determine the correlation between the energy profiles computed with both basis sets. A series of single point calculations at CASSCF(8,8)/3-21G along the CASSCF(8,8)/6-31G* minimum energy path (from S_3 to S_0) have been performed (see Fig 7S). A good (qualitative) agreement between both energy profiles is found.

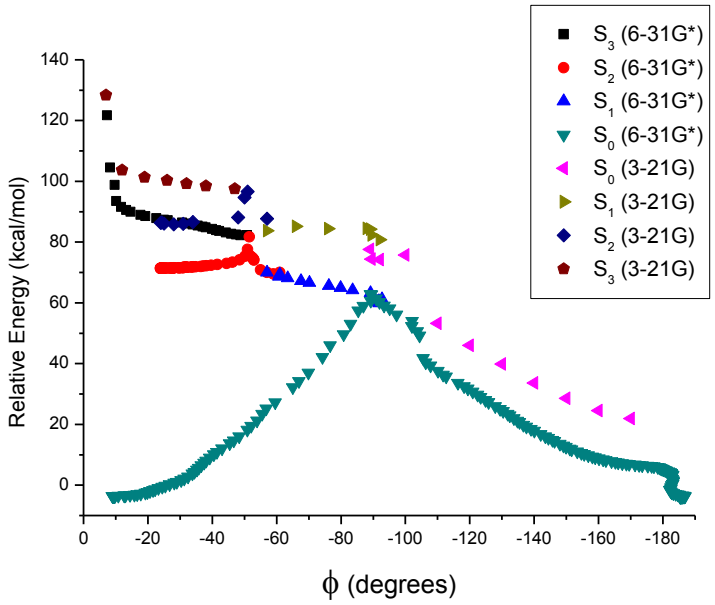

Fig 7S. CASSCF(8,8)/3-21G and CASSCF(8,8)/6-31G* energy profiles along the CASSCF(8,8)/6-31G* minimum energy path (from S_3 to S_0). The energy (vertical axis) is represented taking as a reference the S_0 energy for the ground state equilibrium structure.

In order to provide a quantitative description of the correlation between both 6-31G* and 3-21G energies obtained, a linear regression of both set of energies has been performed (Fig 8S). A good correlation is found with a slope of 1.15 units and r^2=0.91. This correlation supports the qualitative equivalence between molecular dynamics with the two basis sets.

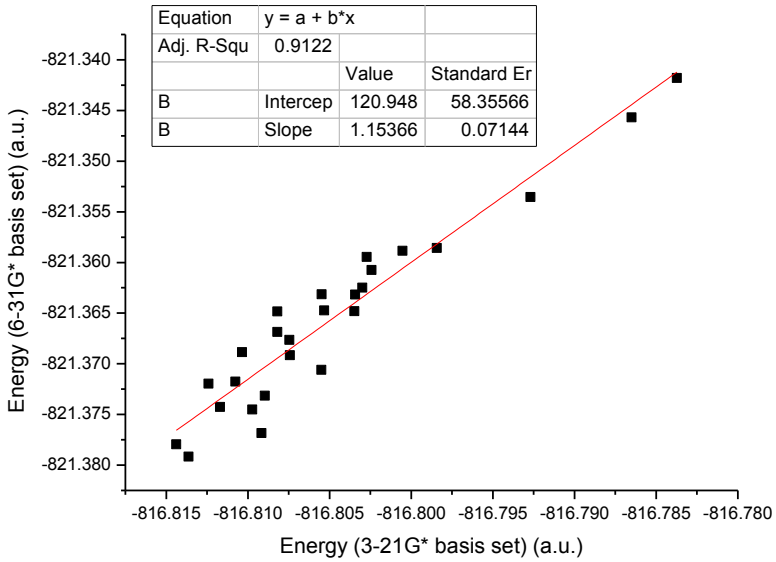

Fig 8S. CASSCF(8,8)/6-31G* vs. CASSCF(8,8)/3-21G energies along the computed minimum energy path (from S_3 to S_0) at the CASSCF(8,8)/6-31G* level. The representation shows a good correlation between both energies, therefore similar shape of the CASSCF(8,8)/3-21G and the CASSCF(8,8)/6-31G* potential energy surfaces is expected.

In conclusion, CASSCF(8,8)/3-21G molecular dynamics are expected to behave similarly (qualitative agreement) to the ones calculated by CASSCF(8,8)/6-31G*, providing the former level of theory a good starting point to rationalize the dynamical behavior of the molecular motor.

9. Nonadibatic CAS(8,8)/3-21G Molecular Dynamics at T=300K.

A series of on-the-fly nonadiabatic molecular dynamics at the CASSCF(8,8)/3-21G level of theory have been performed. Initial conditions were obtained by sampling the phase space for the minimum energy structure on S_0 with 1ns dynamics. The dynamics were performed using a Nose−Hoover chain of thermostats with T=300K.[7-9] The hopping algorithm employed was based on the Landau-Zener formula, where hopping probabilities were calculated for each pass through the intersection space once the two electronic states involved in the crossing are strongly mixed.[2] A total of 20 trajectories were performed up to completeness the decay to the ground state (ranging the simulation times from ca. 0.5 ps to 1.5ps). 4 out of 20 trajectories reached torsions of the central bond larger than 90 degrees in the ground state, evolving on this state in the direction of completing the unidirectional rotation (Fig. 9S).

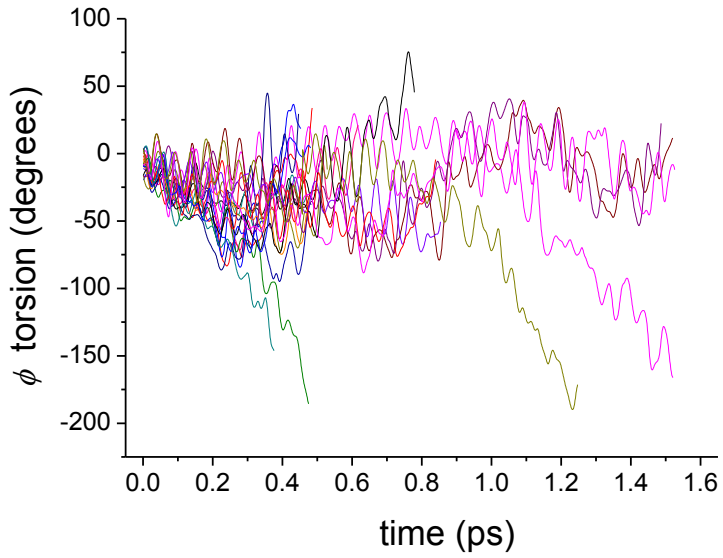

Fig 9S. ϕ central bond torsion angle in degrees vs. the simulation time in picoseconds. After vertical excitation, all trajectories evolve towards the same rotational direction (unidirectional rotation). Also, they evolve to more negative torsions with increasing time, with some of the trajectories (4 out of 20) completing the photoinduced isomerization.

The average lifetime for the S_3 state calculated from the molecular dynamics simulations was ca. 65 fs. On the other hand, the lifetime corresponding to S_2 was ca. 230 fs, while the S_1 state lifetime was estimated to be ca. 33 fs (Fig. 10S). The complete relaxation process is therefore taking place in less than 1 picosecond, and considering an efficiency of at least ca. 20%, it could be possible to have rotation frequencies as high as hundreds of GHz.

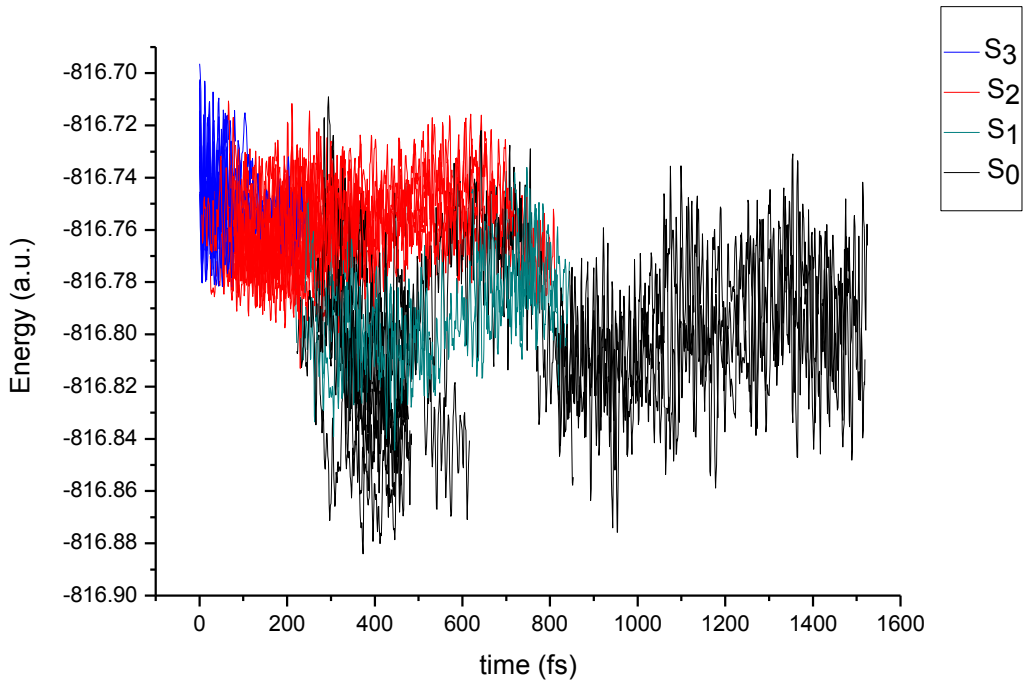

Fig 10S. Energy profile for the computed trajectories reaching the ground state. The different populated electronic states are displayed with diverse colors: S_3 in blue (ca. 65 fs lifetime), S_2 in red (ca. 230 lifetime), S_1 in green (ca. 33fs lifetime) and S_0 in black.

The 6-31G* basis set reference trajectory, even taking place at 0K, implies higher rotational frequency than that found with 3-21G MDs. This is due to the higher steepness character of the potential energy surfaces along the torsion coordinate with 6-31G* than with 3-21G.

Conclusions from CAS(8,8)/3-21G NAMD

In view of the qualitative *CAS(8,8)/3-21G* nonadiabatic molecular dynamics, the proposed photoisomerization mechanism, elucidated by exploring the potential energy surfaces, supports the efficiency of the photoinduced unidirectional rotation for the following reasons:

i) All the computed trajectories rotate in the same unidirectional rotation direction after vertical excitation (decreasing the torsion angle, ϕ).

ii) ca. 20% of the trajectories (4 out of 20) will yield the 180 degrees of rotation.

iii) CASSCF(8,8)/6-31G* (T=0K) provide even higher rotation frequencies, due to the steepness character of the potential energy surfaces along the correct rotation direction which in turn accelerates the rotation motion.

iv) The general picture predicted from MEPs and the analysis of the conical intersections topology is in total agreement with the nonadibatic molecular dynamics simulations: (a) the initial rotation -after vertical excitation- is unidirectional. (b) peaked S_1/S_0 conical intersection is an efficient funnel to the ground state allowing both, the continuation of the torsion in the correct direction and the quenching of the rotation to recover the initial isomer.

10. Cartesian Coordinates of the Most Relevant Molecular Structures.

S_0 MOST STABLE CONFORMATION STRUCTURE

Ground State

C	0.998754	-0.985155	0.308427
C	2.138843	-0.247001	0.179795
C	1.758401	1.143142	-0.092989
C	0.395725	1.231349	-0.112602
C	-0.171438	-0.113538	0.146258
C	-1.470246	-0.545213	0.205593
C	-1.913053	-1.995273	0.193697
C	-3.234517	-1.935237	-0.589484
C	-3.870893	-0.619875	-0.123806
C	-2.687080	0.257685	0.167686
N	-2.803999	1.521965	0.449273
H	-3.726496	1.954655	0.409472
H	-2.008785	2.144287	0.733289
H	-4.422486	-0.764546	0.816571
H	-4.560691	-0.158008	-0.838956
H	-3.878203	-2.797200	-0.401001
H	-3.027955	-1.896060	-1.663238
H	-2.093759	-2.350006	1.217916
H	-1.164000	-2.637054	-0.274201
C	3.375882	-1.079401	0.266781
C	2.809566	-2.405943	0.831700
C	1.299363	-2.441615	0.486754
C	2.436536	2.452306	-0.331790
C	1.252520	3.351760	-0.774226
C	-0.058169	2.631623	-0.374639
H	0.721975	-2.922356	1.290099
O	-0.711498	3.210076	0.794764
O	1.012862	-3.076042	-0.770049
H	-0.818717	2.731342	-1.155933
H	-0.090005	3.127273	1.544637
H	2.919465	-2.408368	1.921325
H	3.324874	-3.290670	0.444119
H	4.153322	-0.652043	0.909272
H	3.817351	-1.209548	-0.729740
H	3.212297	2.394944	-1.103101
H	2.932214	2.814032	0.578773
H	1.268521	3.464412	-1.862019
H	1.278165	4.357141	-0.343697
H	1.227224	-4.023484	-0.676740

S_3/S_2 CONICAL INTERSECTION 51 DEGREES			
C	0.97339	-0.91246	0.43380
C	2.19244	-0.17652	0.26817
C	1.85626	1.11475	-0.11645
C	0.43500	1.16737	-0.28111
C	-0.15963	-0.09748	0.06617
C	-1.58176	-0.54875	-0.02739
C	-1.94009	-1.88150	-0.65270
C	-3.47364	-1.83067	-0.78318
C	-3.93837	-0.73725	0.19612
C	-2.69328	0.08129	0.44380
N	-2.79719	1.29767	1.03046
H	-3.68716	1.62653	1.32808
H	-2.02305	1.90946	1.17011
H	-4.29271	-1.15021	1.13753
H	-4.74320	-0.13311	-0.21071
H	-3.93658	-2.78773	-0.57881
H	-3.74176	-1.55158	-1.79495
H	-1.62618	-2.69454	0.00130
H	-1.44190	-2.05137	-1.60215
C	3.38474	-1.04644	0.49941
C	2.75494	-2.29064	1.17723
C	1.29568	-2.36813	0.67018
C	2.48399	2.44825	-0.37221
C	1.32414	3.23594	-1.04283
C	0.00490	2.58840	-0.56444
H	0.63872	-2.84296	1.38874
O	-0.51269	3.18223	0.60534
O	1.20711	-2.98467	-0.58562
H	-0.77824	2.66345	-1.30177
H	0.18176	3.44990	1.19381
H	2.75591	-2.15705	2.25366
H	3.29889	-3.19991	0.95534
H	4.15368	-0.57133	1.09651
H	3.82541	-1.29682	-0.46213
H	3.36968	2.38929	-0.99281
H	2.79340	2.89121	0.57235
H	1.39776	3.12859	-2.11851
H	1.34473	4.29478	-0.81888
H	1.31678	-3.92365	-0.50346

S2 MINIMUM

C	0.96908	-0.93065	0.26144
C	2.23517	-0.17398	0.20744
C	1.88671	1.13056	-0.01118
C	0.40554	1.16575	-0.09483
C	-0.17550	-0.11084	0.09868
C	-1.55056	-0.55084	0.05322
C	-1.92690	-2.00380	-0.20760
C	-3.40199	-1.91572	-0.62815
C	-3.92618	-0.66275	0.08100
C	-2.69162	0.18786	0.25836
N	-2.84144	1.48288	0.60248
H	-3.75806	1.80701	0.81438
H	-2.10306	2.02589	0.99234
H	-4.34103	-0.89386	1.06006
H	-4.69597	-0.14313	-0.47966
H	-3.96424	-2.80564	-0.37686
H	-3.46416	-1.77767	-1.70166
H	-1.82640	-2.60136	0.69684
H	-1.31216	-2.46452	-0.97036
C	3.40305	-1.09335	0.41112
C	2.72114	-2.33504	1.03886
C	1.29994	-2.39611	0.43884
C	2.45831	2.49152	-0.27532
C	1.26833	3.21234	-0.96354
C	-0.02073	2.58898	-0.39135
H	0.59802	-2.91658	1.07719
O	-0.44460	3.18495	0.81176
O	1.29552	-2.91098	-0.86438
H	-0.85066	2.64653	-1.07640
H	0.28125	3.56113	1.29334
H	2.64881	-2.21009	2.11474
H	3.26587	-3.25231	0.85133
H	4.17231	-0.67465	1.04667
H	3.85563	-1.34033	-0.54353
H	3.34206	2.46844	-0.89886
H	2.73843	2.97606	0.65677
H	1.30222	3.02205	-2.03028
H	1.27574	4.28624	-0.82471
H	1.49398	-3.83963	-0.85018

S_2/S_1 CONICAL INTERSECTION 57 DEGREES			
C	1.06439	-0.95637	0.42234
C	2.22807	-0.20620	0.34050
C	1.84279	1.05669	-0.13714
C	0.42561	1.04620	-0.43729
C	-0.11097	-0.18544	-0.13935
C	-1.50727	-0.64434	-0.08606
C	-2.08798	-1.55969	-1.14670
C	-3.61670	-1.41337	-0.98437
C	-3.83462	-0.76106	0.39515
C	-2.50635	-0.10729	0.68758
N	-2.37670	0.83734	1.63482
H	-3.19648	1.19664	2.07187
H	-1.59047	1.45273	1.63110
H	-4.05222	-1.49522	1.16633
H	-4.64808	-0.04358	0.39440
H	-4.13418	-2.35885	-1.07572
H	-4.00297	-0.75811	-1.75608
H	-1.74799	-2.57806	-0.97751
H	-1.75502	-1.29133	-2.14529
C	3.44176	-1.00860	0.72939
C	2.78971	-2.26900	1.36531
C	1.34236	-2.37793	0.81790
C	2.41147	2.41320	-0.37365
C	1.30605	3.10419	-1.21243
C	-0.02608	2.43357	-0.80705
H	0.65539	-2.74439	1.57440
O	-0.56568	2.99697	0.36922
O	1.23112	-3.13854	-0.35536
H	-0.75563	2.45310	-1.60698
H	-0.86638	3.88189	0.20127
H	2.74707	-2.14439	2.44182
H	3.35223	-3.17182	1.16238
H	4.09321	-0.49602	1.42600
H	4.02812	-1.25922	-0.14742
H	3.37814	2.38680	-0.86296
H	2.55189	2.90344	0.58790
H	1.48636	2.92410	-2.26672
H	1.27987	4.17622	-1.06210
H	1.34809	-4.05991	-0.16151

S_1/S_0 CONICAL INTERSECTION 92 DEGREES			
C	0.96262	-0.90431	0.48025
C	2.14893	-0.21910	0.30731
C	1.84936	1.09929	-0.32720
C	0.52411	1.11035	-0.58638
C	-0.09124	-0.15352	-0.08037
C	-1.48689	-0.54147	-0.16766
C	-2.04191	-1.35388	-1.32832
C	-3.56434	-1.31232	-1.07066
C	-3.74249	-0.95815	0.41866
C	-2.43513	-0.29643	0.78320
N	-2.28827	0.42560	1.91098
H	-3.09172	0.62363	2.46593
H	-1.55091	1.09443	1.98593
H	-3.88780	-1.83995	1.03715
H	-4.58686	-0.29974	0.59247
H	-4.04139	-2.24825	-1.32839
H	-4.01214	-0.53981	-1.68339
H	-1.64248	-2.36226	-1.30283
H	-1.77911	-0.93557	-2.29373
C	3.31860	-1.03381	0.74678
C	2.63497	-2.17661	1.54348
C	1.19857	-2.30806	0.97684
C	2.50640	2.42420	-0.58794
C	1.35321	3.18685	-1.30012
C	0.02720	2.48821	-0.90788
H	0.49183	-2.62274	1.73690
O	-0.53919	2.98055	0.28790
O	1.11813	-3.14030	-0.14945
H	-0.70201	2.53032	-1.70880
H	-0.89989	3.84730	0.14554
H	2.57653	-1.89452	2.58952
H	3.17607	-3.11252	1.48571
H	4.03924	-0.47278	1.33021
H	3.83790	-1.40360	-0.13445
H	3.39233	2.35585	-1.20842
H	2.79607	2.89896	0.34416
H	1.48146	3.10535	-2.37400
H	1.33536	4.24118	-1.05235
H	1.23675	-4.04802	0.10143

S_2 TS from S_2 MINUM ENERGY STRUCTURE			
C	0.96618	-0.95639	0.42360
C	2.17261	-0.17554	0.27914
C	1.84110	1.10709	-0.20160
C	0.47674	1.08928	-0.44626
C	-0.10983	-0.25845	-0.08172
C	-1.52353	-0.66519	-0.09164
C	-2.06103	-1.62270	-1.13867
C	-3.59606	-1.50423	-1.01474
C	-3.86000	-0.78937	0.32593
C	-2.54500	-0.11785	0.64037
N	-2.45949	0.85477	1.56991
H	-3.30516	1.20817	1.95935
H	-1.71449	1.51786	1.53117
H	-4.10494	-1.48885	1.12159
H	-4.67331	-0.07393	0.26432
H	-4.08612	-2.46758	-1.06628
H	-3.98376	-0.90143	-1.82790
H	-1.70133	-2.62874	-0.93166
H	-1.71099	-1.37714	-2.13881
C	3.36274	-0.98578	0.65550
C	2.73563	-2.17949	1.42314
C	1.29952	-2.35603	0.86849
C	2.44649	2.45925	-0.48394
C	1.26401	3.18309	-1.19325
C	-0.03585	2.47223	-0.75459
H	0.62128	-2.72815	1.62761
O	-0.61802	3.01775	0.41236
O	1.25648	-3.16347	-0.27763
H	-0.80411	2.49632	-1.51265
H	0.04606	3.42326	0.95523
H	2.68701	-1.94179	2.48043
H	3.31756	-3.08588	1.31670
H	4.09794	-0.42996	1.22606
H	3.84877	-1.31150	-0.26335
H	3.32334	2.41339	-1.11664
H	2.74136	2.95677	0.43486
H	1.37170	3.06954	-2.26559
H	1.22224	4.24514	-0.98390
H	1.41612	-4.07009	-0.04693

11. References.

(1) Roos, B. O.; Taylor, P. R.; Siegbahn, P. E. M. *Chem. Phys*. **1980**, *48*, 157.

(2) Andersson, K.; Malmqvist, P.-Å.; Roos, B. O. *J. Chem. Phys*. **1992**, *96*, 1218.

(3) Merchán, M.; Serrano-Andrés, L.; Fülscher, M. P.; Roos, B. O. In *Recent Advances in Multireference Theory*; K. H. U., Ed.; World Scientific Publishing Co.: Singapore, 1999; Vol. IV, pp 161-195.

(4) Atchity, G. J., S. S. Xantheas and K. Ruedenberg. *J. Chem. Phys*. **1991** *95*: 1862-1876.

(5) Frisch, M. J.; Trucks, G. W.; Schlegel, H. B.; Scuseria, G. E.;Robb, M. A.; Cheeseman; J. R.; Scalmani; G.; Barone; V.; Mennucci;B.; Petersson, G. A.; Nakatsuji, H.; Caricato, M.; Li, X.; Hratchian, H.P.; Izmaylov, A. F.; Bloino, J.; Zheng, G.; Sonnenberg, J. L.; Hada, M.; Ehara, M.; Toyota, K.; Fukuda, R.; Hasegawa, J.; Ishida, M. N.; Honda, Y.; Kitao, O.; Nakai, H.; Vreven, T.; Montgomery, J. A., Jr.; Peralta, J. E.; Ogliaro, F.; Bearpark, M.; Heyd, J. J.; Brothers, E.; Kudin, K. N.; Staroverov, V. N.; Kobayashi, R.; Normand, J.; Raghavachari, K.; Rendell, A.; Burant, J. C.; Iyengar, S. S.; Tomasi, J.; Cossi, M.; Rega, N.; Millam, J. M.; Klene, M.; Knox, J. E.; Cross, J. B.; Bakken, V.; Adamo, C.; Jaramillo, J.; Gomperts, R.; Stratmann, R. E.; Yazyev, O.; Austin, A. J.; Cammi, R.; Pomelli, C.; Ochterski, J. W.; Martin, R. L.; Morokuma, K.; Zakrzewski, V. G.; Voth, G. A.; Salvador, P.; Dannenberg, J. J.; Dapprich, S.; Daniels, A. D.; Farkas, O.; Foresman, J. B.; Ortiz, J. V.; Cioslowski, J.; Fox, D. J. Gaussian 09, revision B.01; Gaussian, Inc.: Wallingford, CT, **2009**.

(6) Aquilante, F.; De Vico, L.; Ferré, N.; Ghigo, G.; Malmqvist, P.-Å.; Neogrády, P.; Pedersen, T. B.; Pitoňák, M.; Reiher, M.; Roos, B. O.; Serrano-Andrés, L.; Urban, M.; Veryazov, V.; Lindh, R. *J. Comput. Chem*. **2010**, *31*, 224–247.

(7) Martyna, G. J.; Tuckerman, M. E.; Tobias, D. J.; Klein, M. L. *Mol. Phys.* **1996**, *87*, 1117.

(8) Tuckerman, M. E.; Liu, Y.; Ciccoti, G.; Martyna, G. J. *J. Chem. Phys.* **2001**, *115*, 1678.

(9) Tuckerman, M. E.; Martyna, G. J. *The Journal of Physical Chemistry B* **2001**, *105*, 7598.

(10) Wilson, E. B.; Decius, J. C.; Cross, P. C. *Molecular Vibrations: the Theory of infrared and Raman Vibrational spectra*; McGraw-Hill 1955.

(11) Field, M. J. *A Practical Introduction to the simulation of Molecular Systems*; Cambridge University Press: New York, 1999.

(12) Frutos, L. M.; Andruniow, T. ; Santoro, F.; Ferré N. and Olivucci M. *Proceedings of the National Academy of Sciences (PNAS)* **2007**, *104*, 7764